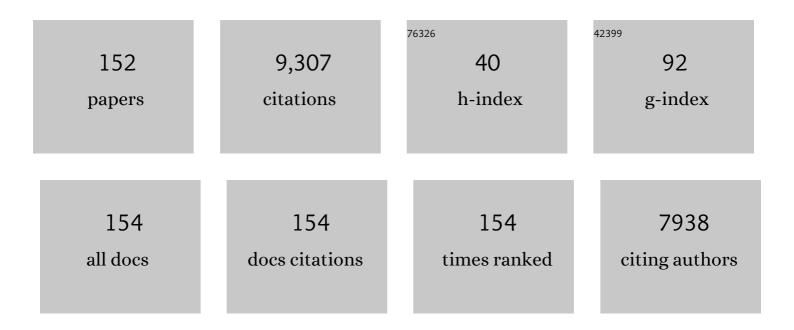
## Wubingfang

List of Publications by Year in descending order

Source: https://exaly.com/author-pdf/261179/publications.pdf Version: 2024-02-01



WURINGEANC

#	Article	IF	CITATIONS
1	Revegetation in China's Loess Plateau is approaching sustainable water resource limits. Nature Climate Change, 2016, 6, 1019-1022.	18.8	1,270
2	Improvements in ecosystem services from investments in natural capital. Science, 2016, 352, 1455-1459.	12.6	1,117
3	Assessing the soil erosion control service of ecosystems change in the Loess Plateau of China. Ecological Complexity, 2011, 8, 284-293.	2.9	681
4	Effects of national ecological restoration projects on carbon sequestration in China from 2001 to 2010. Proceedings of the National Academy of Sciences of the United States of America, 2018, 115, 4039-4044.	7.1	486
5	Carbon pools in China's terrestrial ecosystems: New estimates based on an intensive field survey. Proceedings of the National Academy of Sciences of the United States of America, 2018, 115, 4021-4026.	7.1	466
6	A Policy-Driven Large Scale Ecological Restoration: Quantifying Ecosystem Services Changes in the Loess Plateau of China. PLoS ONE, 2012, 7, e31782.	2.5	392
7	China's wetlands loss to urban expansion. Land Degradation and Development, 2018, 29, 2644-2657.	3.9	244
8	Recent ecological transitions in China: greening, browning and influential factors. Scientific Reports, 2015, 5, 8732.	3.3	189
9	A comparison of global agricultural monitoring systems and current gaps. Agricultural Systems, 2019, 168, 258-272.	6.1	183
10	Conversions between natural wetlands and farmland in China: A multiscale geospatial analysis. Science of the Total Environment, 2018, 634, 550-560.	8.0	173
11	Using NOAA AVHRR and Landsat TM to estimate rice area year-by-year. International Journal of Remote Sensing, 1998, 19, 521-525.	2.9	142
12	Validation of ETWatch using field measurements at diverse landscapes: A case study in Hai Basin of China. Journal of Hydrology, 2012, 436-437, 67-80.	5.4	137
13	30 m Resolution Global Annual Burned Area Mapping Based on Landsat Images and Google Earth Engine. Remote Sensing, 2019, 11, 489.	4.0	122
14	Remote sensing-based global crop monitoring: experiences with China's CropWatch system. International Journal of Digital Earth, 2014, 7, 113-137.	3.9	116
15	Land degradation and restoration in the arid and semiarid zones of China: Quantified evidence and implications from satellites. Land Degradation and Development, 2018, 29, 3841-3851.	3.9	105
16	Altered trends in carbon uptake in China's terrestrial ecosystems under the enhanced summer monsoon and warming hiatus. National Science Review, 2019, 6, 505-514.	9.5	93
17	Towards a set of agrosystem-specific cropland mapping methods to address the global cropland diversity. International Journal of Remote Sensing, 2016, 37, 3196-3231.	2.9	92
18	Generation of high spatial and temporal resolution NDVI and its application in crop biomass estimation. International Journal of Digital Earth, 2013, 6, 203-218.	3.9	91

#	Article	IF	CITATIONS
19	Predicting Wheat Yield at the Field Scale by Combining High-Resolution Sentinel-2 Satellite Imagery and Crop Modelling. Remote Sensing, 2020, 12, 1024.	4.0	89
20	Improving Estimates of Grassland Fractional Vegetation Cover Based on a Pixel Dichotomy Model: A Case Study in Inner Mongolia, China. Remote Sensing, 2014, 6, 4705-4722.	4.0	82
21	Mapping up-to-Date Paddy Rice Extent at 10 M Resolution in China through the Integration of Optical and Synthetic Aperture Radar Images. Remote Sensing, 2018, 10, 1200.	4.0	79
22	Assessment of soil erosion and sediment delivery ratio using remote sensing and GIS: a case study of upstream Chaobaihe River catchment, north China. International Journal of Sediment Research, 2008, 23, 167-173.	3.5	78
23	Crop classification using multi-configuration SAR data in the North China Plain. International Journal of Remote Sensing, 2012, 33, 170-183.	2.9	75
24	Agricultural drought mitigating indices derived from the changes in drought characteristics. Remote Sensing of Environment, 2020, 244, 111813.	11.0	72
25	Global Crop Monitoring: A Satellite-Based Hierarchical Approach. Remote Sensing, 2015, 7, 3907-3933.	4.0	69
26	Variation in actual evapotranspiration following changes in climate and vegetation cover during an ecological restoration period (2000–2015) in the Loess Plateau, China. Science of the Total Environment, 2019, 689, 534-545.	8.0	66
27	Synthesis of global actual evapotranspiration from 1982 to 2019. Earth System Science Data, 2021, 13, 447-480.	9.9	66
28	Identification of priority areas for controlling soil erosion. Catena, 2010, 83, 76-86.	5.0	64
29	Crop planting and type proportion method for crop acreage estimation of complex agricultural landscapes. International Journal of Applied Earth Observation and Geoinformation, 2012, 16, 101-112.	2.8	60
30	Efficient Identification of Corn Cultivation Area with Multitemporal Synthetic Aperture Radar and Optical Images in the Google Earth Engine Cloud Platform. Remote Sensing, 2019, 11, 629.	4.0	57
31	Modeling grassland aboveground biomass using a pure vegetation index. Ecological Indicators, 2016, 62, 279-288.	6.3	56
32	Crop Phenology Detection Using High Spatio-Temporal Resolution Data Fused from SPOT5 and MODIS Products. Sensors, 2016, 16, 2099.	3.8	53
33	Assessing potential water savings in agriculture on the Hai Basin plain, China. Agricultural Water Management, 2015, 154, 11-19.	5.6	49
34	Crop classification using HJ satellite multispectral data in the North China Plain. Journal of Applied Remote Sensing, 2013, 7, 073576.	1.3	48
35	Building a Data Set over 12 Globally Distributed Sites to Support the Development of Agriculture Monitoring Applications with Sentinel-2. Remote Sensing, 2015, 7, 16062-16090.	4.0	47
36	Forest species diversity mapping using airborne LiDAR and hyperspectral data in a subtropical forest in China. Remote Sensing of Environment, 2018, 213, 104-114.	11.0	47

#	Article	IF	CITATIONS
37	An Object-Based Paddy Rice Classification Using Multi-Spectral Data and Crop Phenology in Assam, Northeast India. Remote Sensing, 2016, 8, 479.	4.0	46
38	A new framework to map fine resolution cropping intensity across the globe: Algorithm, validation, and implication. Remote Sensing of Environment, 2020, 251, 112095.	11.0	46
39	Mapping ecosystem services for China's ecoregions with a biophysical surrogate approach. Landscape and Urban Planning, 2017, 161, 22-31.	7.5	45
40	Soil erosion assessment in the Blue Nile Basin driven by a novel RUSLE-GEE framework. Science of the Total Environment, 2021, 793, 148466.	8.0	44
41	The GEOGLAM crop monitor for AMIS: Assessing crop conditions in the context of global markets. Global Food Security, 2019, 23, 173-181.	8.1	43
42	Representation of critical natural capital in China. Conservation Biology, 2017, 31, 894-902.	4.7	41
43	Vegetation classification method with biochemical composition estimated from remote sensing data. International Journal of Remote Sensing, 2011, 32, 9307-9325.	2.9	40
44	Determination of Appropriate Remote Sensing Indices for Spring Wheat Yield Estimation in Mongolia. Remote Sensing, 2019, 11, 2568.	4.0	39
45	Scaling-based forest structural change detection using an inverted geometric-optical model in the Three Gorges region of China. Remote Sensing of Environment, 2008, 112, 4261-4271.	11.0	38
46	Image Segmentation Based on Constrained Spectral Variance Difference and Edge Penalty. Remote Sensing, 2015, 7, 5980-6004.	4.0	35
47	Downstream ecosystem responses to middle reach regulation of river discharge in the Heihe River Basin, China. Hydrology and Earth System Sciences, 2016, 20, 4469-4481.	4.9	35
48	Suitability Assessment of Satellite-Derived Drought Indices for Mongolian Grassland. Remote Sensing, 2017, 9, 650.	4.0	34
49	GCI30: a global dataset of 30 m cropping intensity using multisource remote sensing imagery. Earth System Science Data, 2021, 13, 4799-4817.	9.9	34
50	Estimation and Validation of Land Surface Evaporation Using Remote Sensing and Meteorological Data in North China. IEEE Journal of Selected Topics in Applied Earth Observations and Remote Sensing, 2010, 3, 337-344.	4.9	33
51	Impacts of human activities on the evolution of estuarine wetland in the Yangtze Delta from 2000 to 2010. Environmental Earth Sciences, 2015, 73, 435-447.	2.7	33
52	Cloud services with big data provide a solution for monitoring and tracking sustainable development goals. Geography and Sustainability, 2020, 1, 25-32.	4.3	33
53	Downscaling TRMM Monthly Precipitation Using Google Earth Engine and Google Cloud Computing. Remote Sensing, 2020, 12, 3860.	4.0	32
54	A drought monitoring operational system for China using satellite data: design and evaluation. Geomatics, Natural Hazards and Risk, 2016, 7, 264-277.	4.3	31

#	Article	IF	CITATIONS
55	Assessing factors impacting the spatial discrepancy of remote sensing based cropland products: A case study in Africa. International Journal of Applied Earth Observation and Geoinformation, 2020, 85, 102010.	2.8	31
56	Object-Based Paddy Rice Mapping Using HJ-1A/B Data and Temporal Features Extracted from Time Series MODIS NDVI Data. Sensors, 2017, 17, 10.	3.8	29
5 <b>7</b>	Regional Actual Evapotranspiration Estimation with Land and Meteorological Variables Derived from Multi-Source Satellite Data. Remote Sensing, 2020, 12, 332.	4.0	29
58	Integrated spatial–temporal analysis of crop water productivity of winter wheat in Hai Basin. Agricultural Water Management, 2014, 133, 24-33.	5.6	28
59	An Improved Approach for Estimating Daily Net Radiation over the Heihe River Basin. Sensors, 2017, 17, 86.	3.8	28
60	Basin-wide evapotranspiration management: Concept and practical application in Hai Basin, China. Agricultural Water Management, 2014, 145, 145-153.	5.6	27
61	Mapping and evaluation the process, pattern and potential of urban growth in China. Applied Geography, 2016, 71, 44-55.	3.7	27
62	A method for sensible heat flux model parameterization based on radiometric surface temperature and environmental factors without involving the parameter KBâ^'1. International Journal of Applied Earth Observation and Geoinformation, 2016, 47, 50-59.	2.8	27
63	A trade-off method between environment restoration and human water consumption: A case study in Ebinur Lake. Journal of Cleaner Production, 2019, 217, 732-741.	9.3	27
64	A Synthesizing Land-cover Classification Method Based on Google Earth Engine: A Case Study in Nzhelele and Levhuvu Catchments, South Africa. Chinese Geographical Science, 2020, 30, 397-409.	3.0	27
65	Quantifying global agricultural water appropriation with data derived from earth observations. Journal of Cleaner Production, 2022, 358, 131891.	9.3	27
66	A Method for Deriving the Boundary Layer Mixing Height from MODIS Atmospheric Profile Data. Atmosphere, 2015, 6, 1346-1361.	2.3	26
67	Assessing and Correcting Topographic Effects on Forest Canopy Height Retrieval Using Airborne LiDAR Data. Sensors, 2015, 15, 12133-12155.	3.8	26
68	Quantifying impacts of climate variability and human activities on the hydrological system of the Haihe River Basin, China. Environmental Earth Sciences, 2015, 73, 1491-1503.	2.7	26
69	Mapping Winter Wheat Biomass and Yield Using Time Series Data Blended from PROBA-V 100- and 300-m S1 Products. Remote Sensing, 2016, 8, 824.	4.0	25
70	Tree water-use efficiency and growth dynamics in response to climatic and environmental changes in a temperate forest in Beijing, China. Environment International, 2020, 134, 105209.	10.0	25
71	A method to estimate diurnal surface soil heat flux from MODIS data for a sparse vegetation and bare soil. Journal of Hydrology, 2014, 511, 139-150.	5.4	24
72	Dryland ecosystem dynamic change and its drivers in Mediterranean region. Current Opinion in Environmental Sustainability, 2021, 48, 59-67.	6.3	24

#	Article	IF	CITATIONS
73	Crop Condition Assessment with Adjusted NDVI Using the Uncropped Arable Land Ratio. Remote Sensing, 2014, 6, 5774-5794.	4.0	23
74	A comparison of methods for the measurement of CO <sub>2</sub> and CH <sub>4</sub> emissions from surface water reservoirs: Results from an international workshop held at Three Gorges Dam, June 2012. Limnology and Oceanography: Methods, 2015, 13, 15-29.	2.0	23
75	Comparison of Different Cropland Classification Methods under Diversified Agroecological Conditions in the Zambezi River Basin. Remote Sensing, 2020, 12, 2096.	4.0	22
76	Crop Mapping Using PROBA-V Time Series Data at the Yucheng and Hongxing Farm in China. Remote Sensing, 2016, 8, 915.	4.0	21
77	Comparison of evapotranspiration estimated by ETWatch with that derived from combined GRACE and measured precipitation data in Hai River Basin, North China. Hydrological Sciences Journal, 2011, 56, 249-267.	2.6	20
78	Remote sensing based monitoring of interannual variations in vegetation activity in China from 1982 to 2009. Science China Earth Sciences, 2014, 57, 1800-1806.	5.2	20
79	Assessment of environmentally sensitive areas to desertification in the Blue Nile Basin driven by the MEDALUS-GEE framework. Science of the Total Environment, 2022, 815, 152925.	8.0	20
80	An Interannual Transfer Learning Approach for Crop Classification in the Hetao Irrigation District, China. Remote Sensing, 2022, 14, 1208.	4.0	20
81	Maize acreage estimation using ENVISAT MERIS and CBERS-02B CCD data in the North China Plain. Computers and Electronics in Agriculture, 2011, 78, 208-214.	7.7	19
82	A method for estimating soil moisture storage in regions under water stress and storage depletion: a case study of Hai River Basin, North China. Hydrological Processes, 2011, 25, 2275-2287.	2.6	19
83	Bibliometric analysis of ecosystem monitoring-related research in Africa: implications for ecological stewardship and scientific collaboration. International Journal of Sustainable Development and World Ecology, 2016, 23, 412-422.	5.9	19
84	A Method for Estimating the Aerodynamic Roughness Length with NDVI and BRDF Signatures Using Multi-Temporal Proba-V Data. Remote Sensing, 2017, 9, 6.	4.0	19
85	An Improved Method for Deriving Daily Evapotranspiration Estimates From Satellite Estimates on Cloud-Free Days. IEEE Journal of Selected Topics in Applied Earth Observations and Remote Sensing, 2016, 9, 1323-1330.	4.9	18
86	A Practical Satellite-Derived Vegetation Drought Index for Arid and Semi-Arid Grassland Drought Monitoring. Remote Sensing, 2021, 13, 414.	4.0	18
87	Regional Water Balance Based on Remotely Sensed Evapotranspiration and Irrigation: An Assessment of the Haihe Plain, China. Remote Sensing, 2014, 6, 2514-2533.	4.0	17
88	Spectral Discrimination of Opium Poppy Using Field Spectrometry. IEEE Transactions on Geoscience and Remote Sensing, 2011, 49, 3414-3422.	6.3	16
89	Opium poppy monitoring with remote sensing in North Myanmar. International Journal of Drug Policy, 2011, 22, 278-284.	3.3	16
90	An improved satelliteâ€based approach for estimating vapor pressure deficit from MODIS data. Journal of Geophysical Research D: Atmospheres, 2014, 119, 12,256.	3.3	16

#	Article	IF	CITATIONS
91	Estimating Evapotranspiration from an Improved Two-Source Energy Balance Model Using ASTER Satellite Imagery. Water (Switzerland), 2015, 7, 6673-6688.	2.7	16
92	Identification of Crop Type in Crowdsourced Road View Photos with Deep Convolutional Neural Network. Sensors, 2021, 21, 1165.	3.8	16
93	Modified vegetation indices for estimating crop fraction of absorbed photosynthetically active radiation. International Journal of Remote Sensing, 2015, 36, 3097-3113.	2.9	15
94	Spatiotemporal Analysis of Precipitation in the Sparsely Gauged Zambezi River Basin Using Remote Sensing and Google Earth Engine. Remote Sensing, 2019, 11, 2977.	4.0	15
95	Regional-scale estimation of evapotranspiration for the North China Plain using MODIS data and the triangle-approach. International Journal of Applied Earth Observation and Geoinformation, 2014, 31, 143-153.	2.8	14
96	Spatial and temporal dynamics of forest aboveground carbon stocks in response to climate and environmental changes. Journal of Soils and Sediments, 2015, 15, 249-259.	3.0	14
97	The Optimal Leaf Biochemical Selection for Mapping Species Diversity Based on Imaging Spectroscopy. Remote Sensing, 2016, 8, 216.	4.0	14
98	Satellite-Based Water Consumption Dynamics Monitoring in an Extremely Arid Area. Remote Sensing, 2018, 10, 1399.	4.0	14
99	Performance and the Optimal Integration of Sentinel-1/2 Time-Series Features for Crop Classification in Northern Mongolia. Remote Sensing, 2022, 14, 1830.	4.0	14
100	Hydro-ecological impact of water conservancy projects in the Haihe River Basin. Acta Oecologica, 2012, 44, 67-74.	1.1	13
101	A connectivity-based assessment framework for river basin ecosystem service management. Current Opinion in Environmental Sustainability, 2018, 33, 34-41.	6.3	13
102	Identifying the Links Among Poverty, Hydroenergy and Water Use Using Data Mining Methods. Water Resources Management, 2020, 34, 1725-1741.	3.9	13
103	Land Cover Changes and Drivers in the Water Source Area of the Middle Route of the South-to-North Water Diversion Project in China from 2000 to 2015. Chinese Geographical Science, 2020, 30, 115-126.	3.0	13
104	Indices enhance biological soil crust mapping in sandy and desert lands. Remote Sensing of Environment, 2022, 278, 113078.	11.0	13
105	A Method to Estimate Sunshine Duration Using Cloud Classification Data from a Geostationary Meteorological Satellite (FY-2D) over the Heihe River Basin. Sensors, 2016, 16, 1859.	3.8	12
106	An NDVI-Based Statistical ET Downscaling Method. Water (Switzerland), 2017, 9, 995.	2.7	12
107	Spatiotemporal Analysis of Actual Evapotranspiration and Its Causes in the Hai Basin. Remote Sensing, 2018, 10, 332.	4.0	12
108	Regional Daily ET Estimates Based on the Gap-Filling Method of Surface Conductance. Remote Sensing, 2018, 10, 554.	4.0	12

#	Article	IF	CITATIONS
109	Scale and landscape features matter for understanding the performance of large payments for ecosystem services. Landscape and Urban Planning, 2020, 197, 103764.	7.5	12
110	Approach for Estimating Available Consumable Water for Human Activities in a River Basin. Water Resources Management, 2018, 32, 2353-2368.	3.9	11
111	A method for downscaling daily evapotranspiration based on 30-m surface resistance. Journal of Hydrology, 2019, 577, 123882.	5.4	11
112	Survey of Community Livelihoods and Landscape Change along the Nzhelele and Levuvhu River Catchments in Limpopo Province, South Africa. Land, 2020, 9, 91.	2.9	11
113	Land Use and Land Cover Mapping Using RapidEye Imagery Based on a Novel Band Attention Deep Learning Method in the Three Gorges Reservoir Area. Remote Sensing, 2021, 13, 1225.	4.0	11
114	Enhancing China's Three Red Lines strategy with water consumption limitations. Science Bulletin, 2021, 66, 2057-2060.	9.0	11
115	How long did crops survive from floods caused by Cyclone Idai in Mozambique detected with multi-satellite data. Remote Sensing of Environment, 2022, 269, 112808.	11.0	11
116	Detecting the linkage between arable land use and poverty using machine learning methods at global perspective. Geography and Sustainability, 2022, 3, 7-20.	4.3	11
117	Quantifying winter wheat residue biomass with a spectral angle index derived from China Environmental Satellite data. International Journal of Applied Earth Observation and Geoinformation, 2014, 32, 105-113.	2.8	10
118	Design and characterization of spatial units for monitoring global impacts of environmental factors on major crops and food security. Food and Energy Security, 2016, 5, 40-55.	4.3	10
119	A CNN-Based Self-Supervised Synthetic Aperture Radar Image Denoising Approach. IEEE Transactions on Geoscience and Remote Sensing, 2022, 60, 1-15.	6.3	10
120	Synthesizing a Regional Territorial Evapotranspiration Dataset for Northern China. Remote Sensing, 2021, 13, 1076.	4.0	10
121	An effective biophysical indicator for opium yield estimation. Computers and Electronics in Agriculture, 2011, 75, 272-277.	7.7	9
122	Human Activity Intensity Assessment by Remote Sensing in the Water Source Area of the Middle Route of the South-to-North Water Diversion Project in China. Sustainability, 2019, 11, 5670.	3.2	9
123	Estimating Sunshine Duration Using Hourly Total Cloud Amount Data from a Geostationary Meteorological Satellite. Atmosphere, 2020, 11, 26.	2.3	9
124	Assessing the Impact of Soil on Species Diversity Estimation Based on UAV Imaging Spectroscopy in a Natural Alpine Steppe. Remote Sensing, 2022, 14, 671.	4.0	9
125	A Linear Relationship Between Temporal Multiband MODIS BRDF and Aerodynamic Roughness in HiWATER Wind Gradient Data. IEEE Geoscience and Remote Sensing Letters, 2015, 12, 507-511.	3.1	8
126	Assessment of Agricultural Water Productivity in Arid China. Water (Switzerland), 2020, 12, 1161.	2.7	8

#	Article	IF	CITATIONS
127	Building African Ecosystem Research Network for sustaining local ecosystem goods and services. Chinese Geographical Science, 2015, 25, 414-425.	3.0	7
128	Soil depth spatial prediction by fuzzy soil-landscape model. Journal of Soils and Sediments, 2018, 18, 1041-1051.	3.0	7
129	The Impacts of Vegetation and Meteorological Factors on Aerodynamic Roughness Length at Different Time Scales. Atmosphere, 2018, 9, 149.	2.3	7
130	Coupling water and carbon processes to estimate field-scale maize evapotranspiration with Sentinel-2 data. Agricultural and Forest Meteorology, 2021, 306, 108421.	4.8	7
131	ETWatch cloud: APIs for regional actual evapotranspiration data generation. Environmental Modelling and Software, 2021, 145, 105174.	4.5	7
132	A framework for separating natural and anthropogenic contributions to evapotranspiration of human-managed land covers in watersheds based on machine learning. Science of the Total Environment, 2022, 823, 153726.	8.0	7
133	Method for monitoring environmental flows with high spatial and temporal resolution satellite data. Environmental Monitoring and Assessment, 2022, 194, 13.	2.7	7
134	Quantifying the Contributions of Environmental Factors to Wind Characteristics over 2000–2019 in China. ISPRS International Journal of Geo-Information, 2021, 10, 515.	2.9	6
135	A canopy conductance model with temporal physiological and environmental factors. Science of the Total Environment, 2021, 791, 148283.	8.0	6
136	Soil Erosion and Sediment-Yield Prediction at Basin Scale in Upstream Watershed of Miyun Reservoir. Journal of Hydrologic Engineering - ASCE, 2015, 20, .	1.9	5
137	Land cover mapping and above ground biomass estimation in China. , 2016, , .		5
138	CropWatch agroclimatic indicators (CWAIs) for weather impact assessment on global agriculture. International Journal of Biometeorology, 2017, 61, 199-215.	3.0	5
139	A Refined Crop Drought Monitoring Method Based on the Chinese GF-1 Wide Field View Data. Sensors, 2018, 18, 1297.	3.8	5
140	Constructing a 30m African Cropland Layer for 2016 by Integrating Multiple Remote sensing, crowdsourced, and Auxiliary Datasets. Big Earth Data, 2022, 6, 54-76.	4.4	5
141	Retrieval of key eco-hydrological parameters for cold and arid regions. International Journal of Applied Earth Observation and Geoinformation, 2012, 17, 1-2.	2.8	4
142	Essential dryland ecosystem variables. Current Opinion in Environmental Sustainability, 2021, 48, 68-76.	6.3	4
143	Variations in forest aboveground biomass in Miyun Reservoir of Beijing over the past two decades. Journal of Soils and Sediments, 2017, 17, 2080-2090.	3.0	3
144	Evaluating the Relationship between Field Aerodynamic Roughness and the MODIS BRDF, NDVI, and Wind Speed over Grassland. Atmosphere, 2017, 8, 16.	2.3	3

#	Article	IF	CITATIONS
145	Quantifying the contribution of biophysical and environmental factors in uncertainty of modeling canopy conductance. Journal of Hydrology, 2021, 592, 125612.	5.4	3
146	Spatial Allocation Method from Coarse Evapotranspiration Data to Agricultural Fields by Quantifying Variations in Crop Cover and Soil Moisture. Remote Sensing, 2021, 13, 343.	4.0	3
147	Incorporation of Net Radiation Model Considering Complex Terrain in Evapotranspiration Determination with Sentinel-2 Data. Remote Sensing, 2022, 14, 1191.	4.0	3
148	The improved ET calculation for semiarid region based on an innovative aerodynamic roughness inversion method using multi-source remote sensing data. IOP Conference Series: Earth and Environmental Science, 2014, 17, 012146.	0.3	2
149	Sensitivity of BRDF, NDVI and Wind Speed to the Aerodynamic Roughness Length over Sparse Tamarix in the Downstream Heihe River Basin. Remote Sensing, 2018, 10, 56.	4.0	2
150	The improvement of et calculation in winter by introducing radar-based aerodynamic roughness information into ETWatch system. , 2013, , .		0
151	基于HJ æ~Ÿé«~å‰è°±æ•°æ®çº¢è¾¹åۥ数的冬å°éº¦å¶é¢ç§~æŒ‡æ•°åæ¼". Scientia Sinica Informationis, 2	01d,441, 2	13)220.
152	Method for Environmental Flows Regulation and Early Warning with Remote Sensing and Land Cover Data. Land, 2021, 10, 1216.	2.9	0